Evaluation of Work-Hardening Behavior of HANA TREX Materials

Hyun-Gil Kim*, Il-Hyun Kim, Byung-Kwan Choi, Sang-Yoon Park, Jeong-Yong Park
LWR Fuel Technology Division, 1045 Daedeok-daero, Yuseong-gu, Daejeon, 305-353, Korea
**Corresponding author:hgkim@kaeri.re.kr*

1. Introduction

Zirconium cladding tubes are the first barrier of the fuel in nuclear power plants since they separate the fuel from the cooling environment. The welded tubes could not use in the nuclear system because their properties are non-uniform in the welded area. Thus, non-welded tubes (seamless) have to be applied in this system. Seamless tube can be manufactured by drawing, rolling or pilgering. Among them, the pilgering is the most common production mode for fuel rods, because degree of cold work of more than 80% can be achieved by pilgering process. Therefore, zirconium cladding tubes have been manufactured by a pilgering process from hot extruded billet.

In present time, advanced zirconium alloy have been developed in many countries to meet the economical needs of a PWR's. The advanced zirconium alloys contains a high-Nb as an alloying element when compared to the commercial Zircaloy-4 to improve the corrosion resistance up to high burn-up [1-3]. The tube manufacturing of the high-Nb containing Zr alloy is difficult because the strength of Zr alloy is increased by the solution and precipitation hardening of Nb element in the Zr matrix [4,5]. In addition, the intermediate annealing temperature during tube manufacturing is lower than 610^{o}C to improve the corrosion resistance of the high-Nb containing Zr alloy [4]. Thus, it is anticipated that the tube manufacturing of the high-Nb containing Zr alloy by pilgering process is very difficult. So, it is necessary to investigate the effect of Nb element on the mechanical strength, for manufacturing the high-Nb containing Zr alloy.

Work-hardening is one of the major factors to evaluate the deformation behaviors of metal-based alloys in general. So, the objective of this study is to analyze the work-hardening behaviors of zirconium based alloys containing high-Nb (more than 1.0 wt.%). Also, the microstructural observation and the crystal texture analysis for the tested materials were performed to evaluate the work-hardening mechanism of the zirconium based alloys.

2. Methods and Results

2.1Test and analysis methods

Table 1 shows the chemical compositions of HANA and ZIRLO (as a ref.) alloys. The specimens were cut from the TREX of each alloy, because the pilgering process was started form TREX during the cladding tube manufacturing. The microstructure of TREX was fully re-crystallized state to provide a good deformability of TREX.

Table.1: Chemical composition of zirconium based alloys

Cladding	Alloy Composition (in wt%)					
	Nb	Sn	Fe	Cr	Cu	Zr
HANA-4	1.5	0.4	0.2	0.1	-	Bal.
HANA-6	1.1	-	-	-	0.05	Bal.
ZIRLO	1.0	1.0	0.1	-	-	Bal.

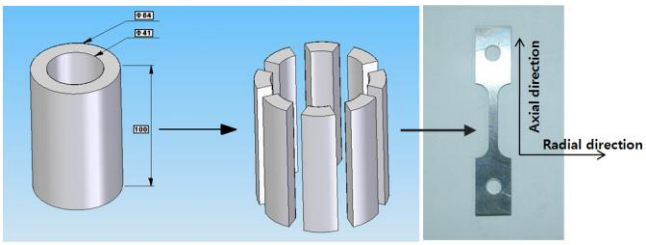

Fig. 1. Schematic drawing of the specimen preparation method for tensile test

Fig. 1 shows the sample preparation method as a dog-born type from TREX. The specimens were tested at room temperature since all of the pilgering processes during the cladding tube manufacturing were performed at room temperature by using the Instron type tensile tester. The tensile test was performed as following the procedure of ASTM E8 – 82 [6]. This test provided information on the strength and ductility of materials under uniaxial tensile stresses. Stress and elongation values were obtained from the attached computer on tester. Several parameters were calculated from the true stress (σ) versus true plastic strain (ε) curve to evaluate the work-hardening behavior. The work-hardening exponent (k) was estimated by fitting a straight line to plots of log σ versus log ε. The stress exponent (n; mean work-hardening rate, $d\sigma/d\varepsilon$) was calculated from the elongation ranges of 0 - 5%. In this work, the repeated tensile tests were applied for the single test specimen to simulate the pilgering process, because the cold working was repeatedly applied on the TREX during the pilgering process. And the elongation at each test was up to 5%.

After the tensile test, the microstructural observation was performed by using the SEM to evaluate the fractured surface and the necking region of the tested samples.

2.2 Tensile test results

Fig. 2 shows the engineering strain-stress curve of HANA-4 TREX material. The number of the repeated tensile test was introduced up to necking of the specimen. From this test result, the YS values were increased with increasing the test cycles, but the UTS values could not see because the elongation of each test was about 5%. Since the uniform elongation was higher than 15% in the commercial Zircaloy-4 which had a re-crystallized microstructure, the UTS peak was not observed in the HANA-4 TREX as well as HANA-6 and ZIRLO TREXs.

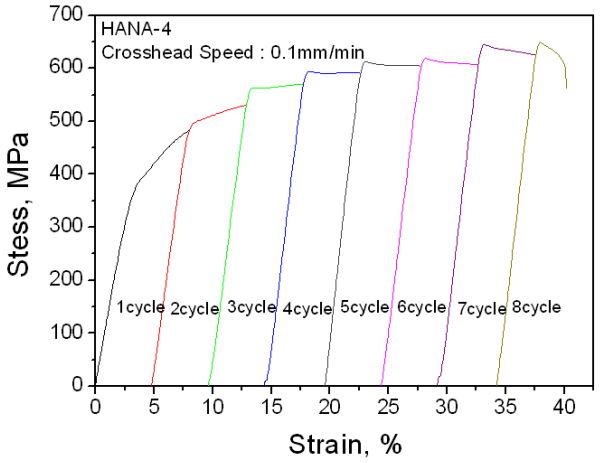

Fig. 2. Engineering strain-stress curves of HANA-4 material after the repeated tensile test at room temperature.

2.3 Work-hardening behavior

The work-hardening behavior of tested alloys was evaluated from the true strain-stress values with the repeated tensile tests. After considering the stress exponent (n), the deformability of three materials was decreased with increasing the repeated tests. Especially, the stress exponent (n) was considerably decreased after 1st tensile test cycle in all materials by work-hardening effects. This is related to the applied dislocations by a plastic strain of 5% at each cyclic test. The stress exponent variation with the cyclic tests was similar in HANA-6 and ZIRLO materials. However, that variation with the cyclic tests was different in HANA-4 material when compared to HANA-6 and ZIRLO. HANA-4 material showed a lower stress exponent with increasing the test cycle than others. From this, it could be recognized that the deformability of HANA-4 was lower than that of HANA-6 and ZIRLO materials.

Fig. 3 shows the SEM images for the necking area after repeated tensile tests. The shear fracture behavior of 45° to the tensile direction was shown in the radial direction of all materials. However, the ductile mode fracture, which could be recognized as a dimple shape, was shown in the central region of fractured surface of all materials.

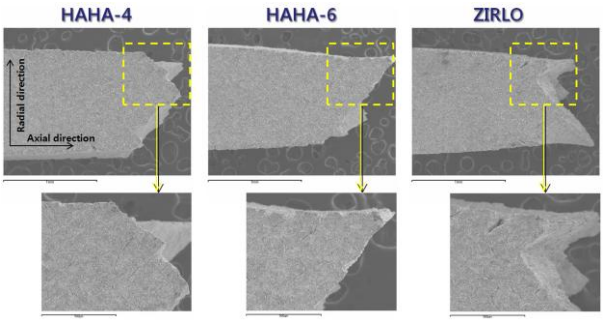

Fig. 3. SEM images for the necking region of the tested materials after the repeated tensile tests.

Thus, the fracture mode of the repeated tensile test was similarly shown when compared to the fracture mode of the single tensile test in zirconium alloys. Since it was observed that area reduction of the HANA-4 was lower than that of the HANA-6 and ZIRLO materials at the necking area, the ductility of HANA-4 after the repeated tensile test condition was decreased when compared to the HANA-6 and ZIRLO materials. This is related to the alloy composition of the material. HANA-4 alloy contained 1.5 wt.% Nb, which was more high content than HANA-6 and ZIRLO as shown in table 1. So, the precipitate hardening effect in HANA-4 is considerably affected on the decrease of ductility during the tensile test.

3. Conclusions

To estimate the work-hardening behavior during the pilgaring process, the repeated tensile test method was applied to the HANA-4, HANA-6, and ZIRLO TREX materials. The stress exponent (n) was considerably decreased after 1st tensile test cycle in all materials by work-hardening effects. After considering the stress exponent (n) and fracture mode, it was known that the ductility of HANA-4 after the repeated tensile test condition was decreased when compared to the HANA-6 and ZIRLO materials.

REFERENCES

[1] R.J. Comstock, G. Schoenberger, G.P. Sabol, Zirconium in the Nuclear Industry, ASTM STP 1295 (1996) 710.
[2] H. Anada, B.J. Herb, K. Nomoto, S. Hagi, R.A. Graham, T. Kuroda, Zirconium in the Nuclear Industry, ASTM STP 1295 (1996) 74. [3] J. H. Baek, Y. H. Jeong, J. Nucl. Mater, 372, 152 (2008).
[3] Y.H. Jeong, S.Y. Park, M.H. Lee, B.K. Choi, J.H. Baek, J.Y. Park, J.H. Kim, H.G. Kim, J. Nucl. Sci. Technol. 43 (2006) 977.
[4] Y.H. Jeong, H.G. Kim, T.H. Kim, J. Nucl. Mater. 317 (2003) 1.
[5] H.G. Kim, J.Y. Park, Y.H. Jeong, J. Nucl. Mater. 347 (2005) 140.
[6] ASTM E8 – 82; Standard methods of tension testing of metallic materials